SCENARIOS FOR BENCHMARKING RANGE-DEPENDENT ACTIVE SONAR PERFORMANCE MODELS

Mario Zampolli, Michael A. Ainslie, Pieter Schippers, TNO Defence Security and Safety, 2509 JG The Hague, Netherlands.
mario.zampolli@tno.nl, michael.ainslie@tno.nl, pieter.schippers@tno.nl

A set of eight sonar problems, pertaining to man-made active sonar, with source frequencies ranging from 250 Hz to 3.5 kHz, is defined. The scenarios are designed to emphasize range dependent propagation aspects in coastal waters, with the aim of testing all terms of the sonar equation (except the detection threshold) both before and after signal processing, including beamforming and matched filtering. The starting point is a range-independent baseline problem, which is a generalization of the Second ONR Reverberation Modeling Workshop problem 'T'. This problem is successively made more complex by adding surface roughness, summer and winter sound speed profiles, deforming the bathymetry into an upslope and a downslope propagation scenario, and by considering the presence of a solitary wave in the water column of the uniform water depth problem. The capability of modelling sub-bottom rough scattering layers and ship noise is also tested in two range-independent problems. A subset of initial results from a first round of comparisons between computations carried out by the participants of the David Weston Memorial Symposium on the Validation of Sonar Performance Assessment Tools, held in Cambridge on 7 – 9 April 2010, is presented.

1 INTRODUCTION

Tactical decision aids, mission planning and design or assessment tools for anti-submarine warfare (ASW) operations employ sonar performance models, with the aim of optimizing sonar use by predicting the detection ranges in a given environment. To achieve this, the individual terms of the sonar equation are modelled, including noise, propagation loss, source level, radiation pattern, and for the active scenarios also target strength, reverberation and return propagation loss. The effect of signal processing on these quantities must also be included in the sonar performance model. Practical models use a number of assumptions to make the calculation more tractable, sometimes at the expense of fidelity. The representation of the environment also differs between models, an example being the representation of rough surface scattering, which can be based for example on empirical Lambert-like scattering rules, or on reflection laws derived from Monte Carlo simulations over different deterministic realizations of a rough surface.

The variety of approaches adopted by the different models calls for a benchmarking effort, which must not only compare the propagation algorithms of the different models, but also the representations of a basic set of signal processing tasks, such as for example beamforming and matched filtering. In response to this need, the Netherlands Organisation for Applied Scientific Research (TNO) has organized a benchmarking effort, which is specifically aimed at comparing different models on low-frequency active sonar (LFAS) scenarios of relevance to shallow water ASW applications, with particular emphasis on range dependence in the environment. This paper presents the definition of the various test scenarios, starting from a baseline range-independent problem, which is obtained as a generalization of the ONR Reverberation Workshop II problem 'T' [1], and evolving gradually towards more complex scenarios with range-dependent bathymetry and sound speed profiles. The purpose of this paper is to describe the test problems, labelled by Roman numerals I – VIII, with the objective of a common platform for the comparison of sonar performance models. The original active LFAS scenarios in the David Weston Memorial Symposium presentations were designated by the labels A2.I – A2.VIII. The new numbering adopted in this paper, using only the Roman numerals, has been adopted for compatibility with future publications.

Section 2 describes the ingredients, such as environmental parameters, source, receiver and target characteristics, from which the individual test problems are obtained. The quantities of interest, requested as outputs from the models, are specified in Section 3. Section 4 contains the descriptions of the individual test problems. Section 5 contains a sample of initial results for problem I, and Section 6 contains the conclusions, which at present are of a preliminary nature.

2 INGREDIENTS OF THE TEST PROBLEMS

2.1 Shallow water waveguides

Two different shallow water waveguide geometries are considered, one range-independent (Figure 1(a)) and the other range-dependent (Figure 1(b)). The range independent geometry applies to problems I – III and VI – VIII, with a granite sub-layer at 5 m depth below the sea floor included in Problem VI.

Unless otherwise stated, the characteristic properties of the water are sound speed c_w = 1500 m/s, density ρ_w□= 1000 kg/m^3, with frequency dependent absorption modelled according to Eq. (1.34) in Ref. [2]. The seabed is assumed to be sand, with sound speed c_b = 1700 m/s, density ratio ρ_b/ρ_w=2 and attenuation β = 0.5 dB per wavelength.

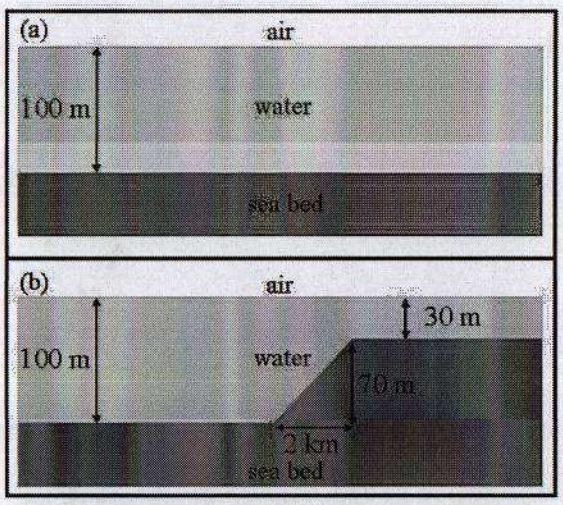

Figure 1: Range independent bathymetry (a), and range dependent bathymetry with a slope of approximately 2 degrees (b).

2.2 Sound speed profiles

In cases for which the sound speed profile in the water column is other than isovelocity at 1500 m/s, two different options are considered (with sound speed interpolated linearly in depth between the defined points):

- An upward refracting linear winter profile, with sound speed at the bottom 1500 m/s and sound speed at the surface 1490 m/s.
- A summer profile with a duct, defined by the (depth, sound speed) pairs: (0 m, 1515.3 m/s), (35 m, 1515.7 m/s), (45 m, 1499.1 m/s), (100 m, 1500 m/s).

2.3 Rough surfaces

The roughness spectrum of the sea floor is given by

$$P(K_x, K_y) = \frac{h^2 l^2}{2\pi(1 + K_x^2 l^2 + K_y^2 l^2)^{3/2}}, \qquad (1)$$

with K_x, K_y being the spatial wavenumbers in the horizontal x-y plane, rms height h = 0.32 m and correlation length l = 400 m [3]. Alternatively, the bottom scattering strength can be modelled by the Lambert rule

$$\mathrm{SS} = -27 + 10\log_{10}\sin\theta_{\mathrm{in}}\sin\theta_{\mathrm{out}} \quad \mathrm{(dB)} \qquad (2)$$

with θ_{in} and θ_{out} representing the incoming and outgoing grazing angles respectively.

In those cases, where a rough sea surface induced by wind is modelled, the wind speed is assumed to be U=10 m/s and the rough surface is modelled by a two-dimensional Pierson-Moskowitz spectrum, as described in Eq. (5) in [5]:

$$P(K_x, K_y) = \frac{\alpha}{4\pi K^4} \exp(-K_L^2 / K^2) \quad (3)$$

where $K^2 = \sqrt{K_x^2 + K_y^2}$, $K_L = \sqrt{0.74}\, g / U^2$, g=9.81 m/s^2 and α= 0.0081. Alternatively, the surface scattering strength can be modelled by the formula

$$\mathrm{SS}(\theta_{in}, \theta_{out}) = \frac{1}{2}[\mathrm{SS}(\theta_{in}) + \mathrm{SS}(\theta_{out})] \ \text{(dB)} \quad (4)$$

using the empirical formula of Chapman and Harris [6]:

$$\mathrm{SS}(\theta) = 3.3\beta \log(\theta/30) - 42.2 \log\beta + 2.6 \ \text{(dB)} \quad (5)$$

In the above equation, $\beta = 158\left(\frac{3600}{1852} U\, f^{1/3}\right)^{-0.58}$, f is the frequency in Hz, θ is the grazing angle in degrees and U=10 m/s.

2.4 Ambient noise model

The ambient noise considered in the test problems is rain noise, represented by a uniform distribution of dipole sources with a spectrum obtained from Eqs. (60) – (63) of Ref. [4] by assuming a rainfall rate of 1 mm per hour and no wind generated noise:

$$\mathrm{NLS}_{\mathrm{rain}} = 41.6 - 10\log_{10} f \ \ \text{(dB re 1μPa}^2\text{/ Hz)} \quad (6)$$

where f is the frequency **in kHz**. Below 0.25 kHz, the rain noise is neglected. Wind noise is neglected in the problems for convenience, since the modelling of a uniform surface noise source is already tested by considering the rain noise.

2.5 Source, receivers and target

Two different types of pulse are considered for the omnidirectional point source, which is located at a depth of SD = 30 m: a Gaussian pulse and a linear frequency modulated (LFM) chirp.
The Gaussian pulses are centred at f_0= 0.25 kHz, f_0 = 1.0 kHz and f_0 = 3.5 kHz, with a -3dB bandwidth of f_0/20, and the corresponding wave forms are defined by:

$$p_{\mathrm{src}}(t) = A\cos(\omega_0 t)\exp\left(-(t\,\Delta\omega)^2/2\right) \quad (7)$$

with $\omega_0 = 2\pi f_0$, $\Delta\omega = \pi\ f_0/20\ [\ln(2)]^{-1/2}$. The values for the pulse amplitude A are 73 kPa for f_0 = 0.25 kHz , 146 kPa for f_0 = 1.0 kHz and 273 kPa for f_0 = 3.5 kHz, all of which yield a source energy level referred to 1 m of 200 dB re μPa^2 s. The Gaussian source pulse is not finite in time, and any numerical representation of it must necessarily cut off at some specified time $t = \pm T_H/2$ around the reference time t = 0 s at which the peak value of the pulse is reached. The cutoff time is here chosen to be the time at which the square of the envelope of the pulse has decayed by about 100 dB relative to the peak value at t = 0 s. For f_0 = 0.25 kHz one obtains $T_H/2$ = 0.1 s (squared envelope of $p_{\mathrm{src}}(t)$ is -96.6 dB relative to the peak amplitude), for f_0 = 1.0 kHz, $T_H/2$ = 0.025 s (squared envelope of $p_{\mathrm{src}}(t)$ is -96.6 dB relative to the peak amplitude), and for f_0 = 3. 5 kHz, $T_H/2$ = 0.007 s (squared envelope of $p_{\mathrm{src}}(t)$ is -92.8 dB amplitude drop).

The LFM chirp is a T_H = 2s upsweep from $f(t_0)$= 1 kHz to $f(t_1)$= 2 kHz, with t_0 = - $T_H/2$ and t_1 = $T_H/2$ denoting start time and the end time of the chirp. The chirp is centred around the time t = 0 s for consistency with the definition of the Gaussian pulse above and for consistency with the matched filter integration described in Sec. 3. Defining the instantaneous frequency slope as s = ($f(t_1)$ - $f(t_0)$)/ (t_1- t_0), the pressure time series of the LFM pulse is given by

$$p_{src}(t) = A\sin\left[2\pi\left(a(t-t_0)+\frac{s}{2}\left(t^2-t_0^2\right)\right)\right] \tag{8}$$

where a= $f(t_0)$ + s $T_H/2$, and A = 10 kPa (which yields a source energy level referred to 1 m of approximately 200 dB re μPa^2 s).

The receivers are arranged in a horizontal line array (HLA), consisting of N = 65 omnidirectional elements. The element spacing Δx is about half a wavelength, namely: Δx = 3.0 m for the Gaussian pulse centred at f_0 = 0.25 kHz, Δx = 0.75 m for f_0 = 1.0 kHz and Δx = 0.20 m for f_0= 3.5 kHz. For the LFM pulse, Δx = 0.375 m, which is a half-wavelength at the highest frequency of the pulse (2 kHz). The array is at a depth of RD = 50 m. (For models requiring a purely monostatic geometry RD = 30 m). The range offset between source and receivers is 0 m, and the HLA is oriented broadside with respect to the target, with the target centre lying in the plane which is perpendicular to the array and passes through the central array hydrophone.

The target is assumed to be a vacuum sphere of a = 5m radius, with an asymptotic limit for the target strength referred to 1 m of TS = 7.96 dB. Assuming a plane wave incident on the sphere parallel to the axis of symmetry, ζ, the target strength at a receiver located at a distance r from the centre of the sphere and at an angle θ relative to the ζ–axis is given by [1]

$$\mathrm{TS} = 10\log_{10}\left(\left|r\ p_{scat}/r_{ref}\right|^2\right) \tag{9}$$

With

$$p_{scat} = \sum_{m=0}^{\infty}(2m+1)i^m P_m(\cos\theta)\frac{j_m(ka)}{h_m(ka)}h_m(kr) \tag{10}$$

In the above equations, r_{ref} = 1m, P_m is a Legendre polynomial of order m, j_m and h_m are the spherical Bessel function of the first kind and the spherical Hankel function respectively, and k is the acoustic wavenumber. Unless otherwise specified, the target centre is at a depth of TD = 10m.

3 QUANTITIES OF INTEREST

Two sets of quantities of interest are defined here for the comparison of the output of sonar performance models. The first set, labelled A.1 – A.6 below, involves model outputs for which no signal processing is considered. The second set, labelled B.1 – B.8 pertains to quantities obtained by passing the model outputs through a broadside beamforming process, and in some cases also through a matched filter. The rationale for the definition of the unprocessed quantities is to enable a comparison of the basic components of the propagation, reverberation, noise and target modelling capabilities of the tools, while the quantities after processing are clearly aimed at comparing the representations of the signal processing chain adopted by the different models.

A quantity frequently used in what follows below, is the **sound pressure level** $L(r,t)$ of an acoustic pressure waveform $p(r,t)$. This is defined as

$$L(r,t) = 10\log_{10}\left[P(r,t)/p_{ref}^2\right], \tag{11}$$

in dB re μPa^2, where

$$P(r,t) = \frac{1}{T_{av}}\int_{t-T_{av}/2}^{t+T_{av}/2} p(r,\tau)^2\,d\tau \tag{12}$$

is the mean-squared value of p over the integration interval of length T_{av} and centred around t. The range parameter r in $p(r,t)$ is the horizontal range of the target relative to the centre of the receive array.

For the pulses defined above, the averaging times to be used are: T_{av} = 15.0 ms for the 0.25 kHz Gaussian pulse,
T_{av} = 3.748 ms for the 1.0 kHz Gaussian pulse,
T_{av} = 1.071 ms for the 3.5 kHz Gaussian pulse and
T_{av} = 2 ms for the LFM chirp.

The averaging times for the Gaussian pulses have been computed using Woodward's effective pulse duration formula [7].

The sound pressure levels at the receivers, obtained by this procedure, are functions of time, t, and of the target range, r, and should be evaluated for r between 1 km and 45 km at increments of 0.1 km. For those models, for which this range sampling is not possible for computational reasons, the results can be computed at a minimal set of ranges: 2.5 km, 5 km, 10 km, 20 km and 40 km.

3.1 Unprocessed outputs

For this portion of the output, no beamforming is considered, and the receiver location is taken to be the centre element of the HLA.

3.1.1 Noise spectral density level, NLS, at the receiver before processing (A.1)

NLS is independent of time and is defined as

$$\mathrm{NLS} = 10\log_{10}\frac{\left\langle P^2\right\rangle_{av}\left(\Delta f\right)_{ref}/\left(\Delta f\right)_{band}}{p_{ref}^2} \tag{13}$$

where p_{ref}^2 = (1 μPa)^2, $\left(\Delta f\right)_{ref}$ = 1 Hz, and $\left(\Delta f\right)_{band}$ is the source signal bandwidth, and where the band-contribution from the noise is given by:

$$\left\langle P^2\right\rangle_{av} = \sum_{n=N}^{M} 2\left|\frac{1}{T}\int_0^T p(r,t)\exp(i2\pi nt/T)\,\mathrm{d}t\right|^2 \tag{14}$$

with p representing the acoustic pressure recorded at the hydrophone output with noise as the only input. The integration time T must be chosen such that $T\left(\Delta f\right)_{band}$ >>1 and the above band-contribution from the noise is stationary with respect to time. The bounds of the summation are N = floor($2T$ times the lowest frequency of the band) and M=ceil($2T$ times the highest frequency of the band). The operations "floor" and "ceil" denote respectively the largest integer bounding the argument from below, and the smallest integer bounding the argument from above.

3.1.2 Echo Level before processing (A.2)

The echo sound pressure level is defined as

$$\mathrm{EL}(r) = 10\log_{10}\left[\max,\, P(r,t)/p_{ref}^2\right] \tag{15}$$

with $t = t_{hp}$ being the time at which the mean squared value of the pressure time series of the echo, $P(r,t)$, computed via Eq. (12), equals its maximum value.

3.1.3 Reverberation Level before processing (A.3)

The reverberation level, RL(r) is defined as the sound-pressure level of the reverberation wave form at the receiver, given by Eqs. (11) and (12), evaluated at time t=t_{hp}.

3.1.4 Signal to reverberation ratio before processing (A.4)

The signal to reverberation ratio before processing, is defined using EL(r), defined in Sec. 3.1.2, and RL(r), defined in Sec. 3.1.3:

$$\mathrm{SRR}(r) = \mathrm{EL}(r) - \mathrm{RL}(r) \tag{16}$$

3.1.5 Propagation loss at different depths (A.5)

An additional quantity of interest, useful for comparing the propagation modules of sonar performance models is the propagation loss, from the sonar source to the target and from the sonar source to a depth of 99m, as a function of the same range bins as those used for the other quantities.

3.1.6 Time dependent sound pressure level of the target echo (A.6)

The sound pressure level of the mean squared echo pressure time series, $P(r,t)$, is

$$\mathrm{SPL}_{\mathrm{echo}}(r,t) = 10\log_{10}\left[P(r,t)/p_{\mathrm{ref}}^2\right] \tag{17}$$

3.2 Processed outputs

Sonar performance models need to represent not only the propagation and scattering physics, but also a signal processing chain. As a basis for comparison between different models, two elementary processing steps are defined here. The output of a broadside beamforming, $b(t)$, for the HLA described in Sec. 2.5, is defined as:

$$b(t) = \frac{1}{N}\sum_{n=1}^{N}\frac{p_n(t)}{p_{\mathrm{ref}}} \tag{18}$$

with $p_n(t)$ being the pressure time series received at the n-th hydrophone.
The second processing step is a *matched filtering of the beamformer output* $b(t)$, with the source signal replica $\sigma(t)=p_{\mathrm{src}}(t)/A$, where $p_{\mathrm{src}}(t)$ and A for the various pulses is defined in Sec. 2.5:

$$m(t) = \int_{-T_H/2}^{T_H/2} b(\tau)\sigma(t+\tau)\mathrm{d}\tau \tag{19}$$

The mean squared beamformer output, $B(r,t)$ is defined by replacing $p(r,t)$ in Eq. (12) with $b(r,t)$. The interpretation of the range parameter is as described in Sec. 3.

3.2.1 Echo level after beamforming (B.1)

The first step in evaluating the echo level after beamforming is the evaluation of Eq. (18), in which $p_n(r,t)$ is the pressure time series containing the echo of the target at horizontal range r, received at the n-th hydrophone. The resulting beamformer output is $b(r,t)$. The echo level after beamforming is thus

$$\mathrm{EL}_{\mathrm{bf}}(r) = 10\log_{10}\max_t B(r,t) \tag{20}$$

The time at which $B(r,t)$ is maximal is denoted by $t = t_{\mathrm{bf}}$.

3.2.2 Reverberation level after beamforming (B.2)

The reverberation level after beamforming, $\mathrm{RL}_{\mathrm{bf}}(r)$, is the beamformer output $B(r,t)$, evaluated at time $t=t_{bf}$, for pressure times series of reverberation only (*i.e.* no target present).

3.2.3 Noise spectral density level after beamforming (B.3)

The noise spectral density level after beamforming, $\mathrm{NLS}_{\mathrm{bf}}$, is obtained by replacing $p(r,t)$ with $b(r,t)\cdot p_{\mathrm{ref}}$ in Eq. (13), and P with B in Eqs. (13) and (14).

3.2.4 Signal to reverberation ratio after beamforming (B.4)

The signal to reverberation ratio after beamforming is

$$\mathrm{SRR}_{\mathrm{bf}}(r) = \mathrm{EL}_{\mathrm{bf}}(r) - \mathrm{RL}_{\mathrm{bf}}(r) \tag{21}$$

3.2.5 Echo level after the matched filter (B.5)

The echo level after the matched filter is

$$\mathrm{EL}_{\mathrm{mf}}(r) = 10\log_{10}\left[\mathrm{average}_t M(r,t)\right] \tag{22}$$

where the average is computed over a time interval of length T_H, around the time $t = t_{\mathrm{mf}}$ at which $M(r,t)$ reaches its maximum value. $M(r,t)=| m(r,t)+ i\,\mathrm{H}(m(r,t))|^2$, with $m(r,t)$ being the matched filter output of Eq. (19), and H being the Hilbert transform. In this particular case, the pressure signal used as an input to the beamformer, which is applied before the matched filter, is the target echo excluding the noise and the reverberation.

3.2.6 Reverberation level after the matched filter (B.6)

The reverberation level after the matched filter is:

$$\mathrm{RL}_{\mathrm{mf}}(r) = 10\log_{10}\left[\mathrm{average}_t M(r,t)\right] \tag{23}$$

with $M(r,t)$ defined as in Sec. 3.2.5, using the pressure time series of reverberation only as an input to the beamformer. The average is computed over the interval of length T_H around time $t = t_{\mathrm{mf}}$.

3.2.7 Noise level after the matched filter (B.7)

The noise level after the matched filter, $\mathrm{NL}_{\mathrm{mf}}$, is obtained by replacing $p(r,t)$ with $m(r,t)\,p_{\mathrm{ref}}$ in Eq. (13), and P with M in Eqs. (13) and (14), where $m(r,t)$ is the matched filter output obtained using the beamformed noise time series as an input.

3.2.8 Signal to noise ratio after the matched filter (B.8)

The signal to noise ratio after the matched filter is

$$\mathrm{SNR}_{\mathrm{mf}}(r) = \mathrm{EL}_{\mathrm{mf}}(r) - 10\log_{10}\left(10^{\mathrm{RL}_{\mathrm{mf}}(r)/10} + 10^{\mathrm{NL}_{\mathrm{mf}}/10}\right) \tag{24}$$

4 SPECIFICATION OF THE TEST PROBLEMS

The test problems are specified using the components defined in Secs. 2 – 3. Unless otherwise specified, the source, target and receiver are as described in Sec. 2.5. The horizontal range, r, of the target relative to the centre of the array goes from 1 km to 45 km, at increments of 0.1 km. For those models, for which this range sampling is not possible for computational reasons, the results can be computed at a minimal set of ranges: 2.5 km, 5 km, 10 km, 20 km and 40 km. The quantities of interest sought are A.1-A.6 and B.1-B.8, defined in Sec. 3.

4.1 Problem I: Range independent, rough bottom

This baseline test case is a generalization of the ONR Reverberation Workshop Problem 'T'. The waveguide of Fig. 1(a), with the isovelocity sound speed profile, is considered. The bottom is rough, according to Sec. 2.3, and the ambient noise (rain noise) is defined as in Sec. 2.4. The sea surface is flat.

4.2 Problem II: Problem I with rough sea surface, no rain

Problem I is extended by including a rough sea surface, induced by a 10 m/s wind. The roughness spectrum and the scattering for this case are defined in Sec. 2.3. The wind noise is taken from Eqs. (58) and (59) in Ref. [4],

$$\mathrm{NLS}_{\mathrm{wind}} = 41.2 + 22.4 \log_{10} U - 15.9 \log_{10} f \qquad (25)$$

in (dB re 1μPa^2 / Hz), with U=10 m/s wind speed and f being the frequency in kHz. For this problem only, the rain noise is disregarded, since a surface noise is already modelled by considering the wind noise. This is the only problem for which wind noise is included. For 250 Hz, wind noise is excluded and the background then consists of reverberation only.

4.3 Problem III: Problem I with winter and duct profiles

The scattering from a rough bottom and a rough sea surface is tested in Problem II, and hence this problem goes back to the flat surface of Problem I. Two sub-cases are defined, to test range-independent, but depth-dependent sound speed profiles.

Subcase 1, is the upward refracting winter profile of Sec. 2.2.

Subcase 2, is the profile with a surface duct defined in Sec. 2.2. Two target depths are to be considered for this subcase: (1) TD = 10m, above the thermocline and (2) TD = 50m, below the thermocline.

4.4 Problem IV: Range dependent bathymetry, upslope case

For this problem, the waveguide geometry is given by Fig. 1(b). The rough seabed is the same as the one defined in Problems I and III, as well as the rain noise. The sound speed profile is the ducted profile of Problem III, Subcase 2 (see Sec. 2.2). For those parts of the waveguide where the water depth is less than 100 m, the sound speed profile at a given range is obtained by evaluating the same function of depth used for the 100 m deep water, with the evaluation terminating at the depth of the sea floor. The horizontal sound speed gradient in the water is therefore zero. The sound speed in water evaluated at the water-sediment boundary is a function of range. The sound in the sediment is independent of range, which means that the critical angle varies with range. The target depth remains as specified in Sec. 2.5. Three subcases are considered.

Subcase 1: The source and receiver array are in 100 m deep water at 5 km range from the downslope extremity of the slope (*i.e.* point at which the slope joins with the 100 m deep waveguide), with the depths specified as in Problem I. The target range locations relative to the source are: from 1 km to 45 km from the source in the upslope direction, at increments of 0.1 km. If, for computational reasons, this sampling should be too demanding, the results can be computed at a minimal set of ranges from the source in the upslope direction: 2.5 km (half way between the source and the slope), 6 km (half way up the slope), 10 km and 30 km.

Subcase 2: The source is fixed in the same location as in subcase 1, and the target is at a range of 6 km from the source, half way up the slope. The target depth is varied from 10 m to 55 m at 5 m increments.

Subcase 3: The target is fixed in the 30 m deep waveguide, at a range of 5 km from the upslope extremity of the slope, at a depth of 10 m. The source is in 100 m deep water, at a range of 5 km from the point at which the wedge joins with the 100 m deep waveguide. The source and receiver depths are the same as in Problem I. The source and receiver are moved away from the wedge (in the downslope direction) at increments of 0.1 km, up to a range of 45 km from the downslope extremity of the slope. If, for computational reasons, this sampling should be too demanding, the results can be computed at a minimal set of ranges from the range where the 100 m deep waveguide joins with the wedge: 5 km, 10 km, 30 km and 40 km.

4.5 Problem V: Range dependent bathymetry, downslope case

In this problem, the locations of the target and receiver relative to the wedge are swapped with respect to Problem IV, so that the propagation from the source to the target is in the downslope direction. The bathymetry and the environmental parameters are the same as those defined in Problem IV. Also in this case, three subcases are considered.

Subcase 1: The source is in 30 m deep water, at 5 km from the upslope extremity of the slope. The source and receiver depths are 15 m in this case. The target depth remains unchanged with respect to Problem III, namely 10 m. The target range locations relative to the source, which are to be used for reporting all the requested results, become: from 1 km to 45 km from the source in the downslope direction, at increments of 0.1 km. If, for computational reasons, this sampling should be too demanding, the results can be computed at a minimal set of ranges from the source in the upslope direction: 2.5 km (half way between the source and the slope), 6 km (half way down the slope), 10 km and 30 km.

Subcase 2: The source is in the same location as in subcase 1. Two different target ranges are considered, one half way down the slope at 6 km from the source, and one in the 100 m deep part of the waveguide at a range of 20 km from the source. For the target at 6 km from the source, the target depth is varied from 10 m to 55 m at 5 m increments. For the target at 20 km from the source, the target depth is varied from 10 m to 90 m at 5 m increments.

4.6 Problem VI: Problem I, no rain, flat bottom, rough sub-bottom layer

This problem is again range independent, and aims at verifying the capability of modelling a layered seabed. The waveguide geometry is the one defined in Fig. 1(a), and the problem definition is obtained from Problem I by considering a flat sea floor, leaving the acoustical properties of the sea floor unchanged. A granite layer of infinite depth is situated below the sea floor, at a depth of 5 m. The acoustical properties of the granite are: density = 2600 kg/m^3, compressional sound speed = 5500 m/s, shear sound speed = 2400 m/s, compressional wave attenuation = 0.15 dB per wavelength, and shear wave attenuation = 0.09 dB per wavelength. The surface roughness of the granite layer is the same as the surface roughness of the sandy bottom used in Problem I. No rain noise is to be considered for this problem. All other parameters are the same as in Problem I.

4.7 Problem VII: Problem I, no rain, ship noise (towship)

The aim of this test case is to verify the modelling of a ship noise. The geometry chosen corresponds to that of a tow-ship. Problem VII is obtained from Problem I by considering no rain noise, and by modelling the towship as a **monopole source at 6 m** depth [8], at a horizontal distance of 300m relative to the source, perpendicular to the plane defined by the source, the central hydrophone of the array and the target. The source and the central hydrophone of the receive array are thus considered to be at the same horizontal distance from the towship. The ship noise is modelled as a **superposition of continuous wave (CW) sinusoids with uniformly distributed random phase**. The monopole source spectrum level of the ship noise function is taken from the paper of Wales and Heitmeyer [8]:

$$S(f) = 230.0 - 10\log_{10}\left(f^{3.594}\right) + 10\log_{10}\left(\left(1+(f/340)^2\right)^{0.917}\right) \qquad (26)$$

in units of dB re μPa²/Hz, scaled to a reference distance of 1 m, with f being the acoustic frequency in hertz. Although the spectrum given by Wales and Heitmeyer is compared to merchant ship data only up to 1200 Hz, the above expression for $S(f)$ is adopted to model the ship source spectrum up to the maximum frequency of interest (*i.e.* 3500 Hz). Spectral lines commonly associated with ship noise are deliberately ignored here.

4.8 Problem VIII: Problem I, no rain, solitary wave

This test problem looks at the capability for modelling a range dependent sound speed, such as the one induced by a solitary wave, or by a train of solitary waves. The definition of this problem still has to be completed, pending the availability of a realistic model for the solitary wave disturbance, which is also sufficiently straightforward to be handled by most sonar performance models.

5 INITIAL RESULTS

As an example, initial results from two models are presented here for Problem I (Sec. 4.1), for the Gaussian source pulse at 1000 Hz centre frequency (Sec. 2.5). The first model is the TNO sonar performance prediction model Almost [9] and the second model is Insight, developed at BAE Systems [10].

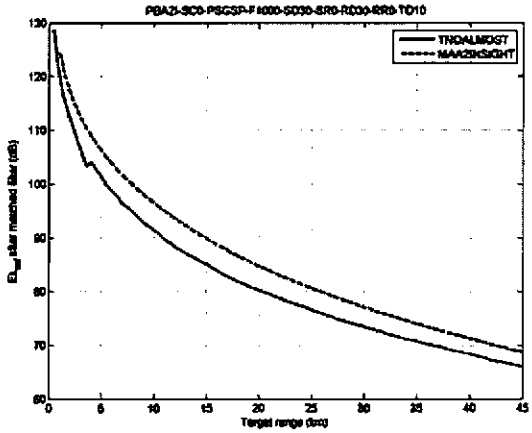

Figure 2: Echo level after the matched filter for Problem I, 1000 Hz Gaussian pulse. Monostatic case.

Figure 2 shows the Echo Level after the beamformer and matched filter (B.5), defined in Sec. 3.2.5, computed for the monostatic case (source depth = receiver depth = 30m), which shows a difference between the two models of less than 5 dB. For the remaining two frequencies, the echo level after matched filter curves produced by the two models show a similar agreement.

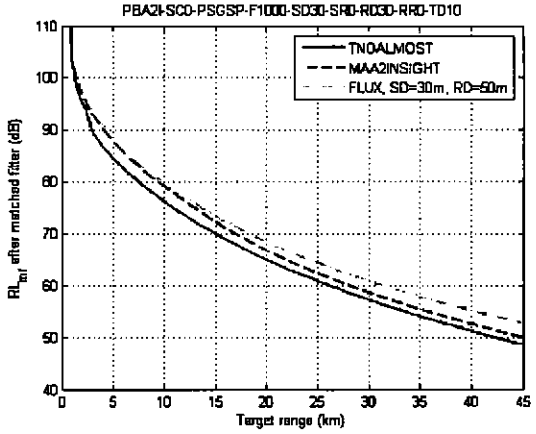

Figure 3: Reverberation level after the matched filter, Problem I, 1000 Hz Gaussian pulse. Monostatic case and comparison to bistatic benchmark result. The bistatic reverberation curve computed with Almost is indistinguishable from the monostatic one on this figure, and it is hence not shown.

The reverberation level after the matched filter (B.6), defined in Sec. 3.2.6, computed also in this case for the monostatic geometry, shows a close agreement between the two models, to within less than 3 dB. Also in this case, the trend for the other Gaussian pulse frequencies is similar to the trend seen in the 1000 Hz case.

A benchmark solution for the reverberation level in the scenario of Problem I (with receiver depth = 50 m) is available in the literature [11], referred to here as "bistatic" to indicate the offset in depth of the receiver relative to the source (the range offset is zero). The benchmark, obtained with the ray-flux based model FLUX, applies to reverberation before any processing and thus should be compared to the model predictions, also before processing. As we do not yet have such a comparison available, as a compromise we subtract the quantity $10\log_{10}N$ from the benchmark curve with $N = 65$, and plot the result as the dash-dotted green line in Figure 3, alongside the predictions of Almost and Insight.
The bistatic solution computed with Almost is found to be indistinguishable from the monostatic one in the Figure, which confirms that the comparison between monostatic and bistatic reverberation solutions is appropriate in this case. The solutions agree with the benchmark result, after the $10\log_{10}N$ correction, to within 4 dB.

6 CONCLUSIONS

Sonar performance models need to calculate each individual term of the sonar equation, including terms representing the processing gain. In order to keep the computational problem a tractable one, the models must necessarily make a number of assumptions and simplifications. This calls for a benchmarking effort, aimed at verifying the reliability and the accuracy of the necessary approximations. Establishing a common platform on which such a comparison can be carried out is a complex task, which is addressed by this paper.

A number of test problems has been defined, covering range-independent as well as range-dependent cases, with increasing degrees of complexity. The scenarios pertain to active ASW applications. A variant of the range-independent problem 'T' from the ONR Reverberation Workshop Series [1] is used as the baseline case. The terms of the sonar equation are tested before processing, and after a basic broadside beamformer and matched filter, which represent the basic components of a processing chain.

Initial results for one of the test problems show fairly good agreement between two models on the echo level and the reverberation level after processing. The reverberation result agrees to within 4 dB with a published reference solution, after correcting for beamforming by subtracting $10\log_{10}N$ from the benchmark curve, where N is the number of hydrophones. The contributions from a larger numbers of models will be compared in future work.

7 ACKNOWLEDGEMENTS

The authors thank Dale Ellis of DRDC Canada for useful comments and for spotting several inconsistencies in the early versions of the test problem descriptions. This work was sponsored by the Defence Research and Development Department of the Netherlands Ministry of Defence.

8 REFERENCES

1. ftp://ftp.ccs.nrl.navy.mil/pub/ram/RevModWkshp_II/Problem_T/Problem_T_22APR08.pdf (Last viewed 26 May 2010).
2. F.B. Jensen, W.A. Kuperman, M.B. Porter, H. Schmidt, *Computational Ocean Acoustics*, Springer-Verlag, New York (2000).
3. ftp://ftp.ccs.nrl.navy.mil/pub/ram/RevModWkshp_I/Problem_Definition_Documents/Environment_040706.pdf (Last viewed 26 May 2010).
4. *APL-UW High-Frequency Ocean Environmental Acoustic Models Handbook*, Technical Report APL-UW TR9407, AEAS 9501, Applied Research Laboratory, University of Washington, Seattle (1994).
5. ftp://ftp.ccs.nrl.navy.mil/pub/ram/RevModWkshp_I/Problem_Definition_Documents/Scattering_models5.pdf (Last viewed 26 May 2010).
6. R.P. Chapman, J.H. Harris, "Surface Backscattering Strengths Measured with Explosive Sound Sources," *J. Acoust. Soc. Am.* **34**, 1592 – 1597 (1962).
7. P.M. Woodward, Probability and Information Theory with Applications to Radar, 2nd Ed., Pergamon Press, Oxford (1964).
8. S.C. Wales, R.M. Heitmeyer, "An ensemble source spectra model for merchant ship-radiated noise," *J. Acoust. Soc. Am.* **111**, 1211 – 1231 (2002).
9. P. Schippers, S.P. Beerens, "Documentation of ALMOST, a model for range dependent propagation and sonar performance predictions," *TNO Report, FEL-98-A126*, TNO, The Hague (1999).
10. M. A. Ainslie, C. H. Harrison, P. W. Burns, "Signal and reverberation prediction for active sonar by adding acoustic components," *IEEE Proc.-Radar, Sonar Navig.* 143 (3), 190-195 (1996).
11. M.A. Ainslie, W. Boek, P.L. Nielsen, C.H. Harrison, "The role of benchmarks in the inversion of low-frequency bottom reverberation," *Proc. Underwater Acoustic Measurements UAM 2007*, Heraklion (2007).

Proceedings of the Institute of Acoustics

NORMAL MODE AND RAY PREDICTIONS FOR THE SONAR PERFORMANCE ASSESSMENT PROBLEMS

Dale D Ellis, DRDC Atlantic, Canada
Email: dale.ellis@drdc-rddc.gc.ca

Two models have been developed for computing reverberation and target echo. The first is a normal mode model, suitable for computing long-range boundary reverberation in a waveguide. The interface scattering and target echo are handled using ray-mode analogies and empirical scattering functions. Time dependence is handled approximately using modal group velocities. The second model is a straight-line ray-trace model, suitable for short times. In addition to reverberation, it includes the fathometer returns since they typically dominate the reverberation in this region. Both models can be applied to the low-frequency active sonar problem from the Symposium on Validation of Sonar Performance Assessment Tools. The ray-trace model is also suitable for the orca-salmon high-frequency short-range sonar problem. Initial predictions for reverberation and target echo will be presented at the Symposium, for comparison with the results from other participants.

Proceedings of the Institute of Acoustics

CALCULATIONS ON PREDEFINED LFAS TEST CASES USING THE ALMOST MODEL FOR PROPAGATION, REVERBERATION, ACTIVE SONAR PERFORMANCE AND COHERENT TARGET SCATTERING

P Schippers, TNO Defence, Security and Safety
email: Pieter.schippers@tno.nl

Since the nineties active and passive sonar performance modelling was developed in the ALMOST propagation model of TNO Defence, Security and Safety. Active detection performance was started for point targets of given Target Strength. Within the Torpedo Defence System TestBed (TDSTB), developed at TNO, with ALMOST as acoustic kernel, there was a demand for TS of target objects and ship wakes. This resulted in coherent target modelling based on the (time domain) impulse response function for a target built up from scattering pixels. Also semi transparent wall structures are taken into account assuming extra pixel layers. By FFT towards the frequency domain any pulse type and signal processing is optional to obtain time series for target echo structures including detector modelling. Reverberation is modelled with various options, like using scattering curves taken from the implemented data base, or using Lamberts law parameters, or from computations for scattering surfaces with given spatial roughness spectra, applying here the described coherent target modelling method to bottom samples too. Beamforming is standard or can optionally be made afterwards using coherently modelled hydrophone signals from the receiver array. The propagation module can optionally apply MGS bottom loss algorithms, but it works preferably with a sediment propagation module. All predefined test cases are in essence compatible with the standard ALMOST input, and results will be made available.

ENERGY FLUX PREDICTIONS FOR THE SONAR PERFORMANCE ASSESSMENT PROBLEM T

Charles W. Holland
The Pennsylvania State University, Applied Research Laboratory, State College, PA, USA

David Weston made substantial contributions to our understanding of acoustic propagation in the ocean through development of energy flux techniques. His work permitted deeper insight into fundamental relationships, for example, the ray invariant, that can be applied to understanding spatial and temporal behavior of propagation and reverberation. An energy flux model based on Weston's pioneering work will be used to address the target sphere problem (Problem T). The modeling will explore the role (turns out to be minor for this problem) of the beam displacement of the seabed reflected component. Situations in which the beam displacement would be expected to be important, will be briefly explored. Initial predictions for reverberation and target echo will be presented at the Symposium, for comparison with the results from other participants.